59. M. Lane, D.K. Gardner, Mitochondrial malate-aspartate shuttle regulates mouse embryo nutrient consumption. *J Biol Chem* 280, 18361-18367 (2005).

60. R. Dumollard, K. Campbell, G. Halet, J. Carroll, K. Swann, Regulation of cytosolic and mitochondrial ATP levels in mouse eggs and zygotes. *Dev Biol* 316, 431-440 (2008).

61. C.F. Rosenkrans, Jr., G.Q. Zeng, M.C. GT, P.K. Schoff, N.L. First, Development of bovine embryos *in vitro* as affected by energy substrates. *Biol Reprod* 49, 459-462 (1993).

62. Y. Takahashi, N.L. First, *In vitro* development of bovine one-cell embryos: Influence of glucose, lactate, pyruvate, amino acids and vitamins. *Theriogenology* 37, 963-978 (1992).

63. M.B. Dworkin, E. Dworkin-Rastl, Metabolic regulation during early frog development: flow of glycolytic carbon into phospholipids in Xenopus oocytes and fertilized eggs. *Dev Biol* 132, 524-528 (1989).

64. M.B. Dworkin, E. Dworkin-Rastl, Regulation of carbon flux from amino acids into sugar phosphates in Xenopus embryos. *Dev Biol* 138, 177-187 (1990).

65. M.B. Dworkin, E. Dworkin-Rastl, Carbon metabolism in early amphibian embryos. *Trends Biochem Sci* 16, 229-234 (1991).

66. T. Ureta, W.Y. Fernandez, J.J. Centelles, M. Cascante, In vivo measurements of control coefficients for hexokinase and glucose-6-phosphate dehydrogenase in Xenopus laevis oocytes. *FEBS Lett* 475, 145-149 (2000).

67. A. Preller, V. Guixe, T. Ureta, In vivo operation of the pentose phosphate pathway in frog oocytes is limited by NADP+ availability. *FEBS Lett* 446, 149-152 (1999).

68. W. Ying, NAD+/NADH and NADP+/NADPH in cellular functions and cell death: regulation and biological consequences. *Antioxid Redox Signal* 10, 179-206 (2008).

69. L. Covarrubias, D. Hernandez-Garcia, D. Schnabel, E. Salas-Vidal, S. Castro-Obregon, Function of reactive oxygen species during animal development: passive or active? *Dev Biol* 320, 1-11 (2008).

70. O. Coll, A. Morales, J.C. Fernandez-Checa, C. Garcia-Ruiz, Neutral sphingomyelinase-induced ceramide triggers germinal vesicle breakdown and oxidant-dependent apoptosis in Xenopus laevis oocytes. *J Lipid Res* 48, 1924-1935 (2007).

71. Y. Zhou, C. Ma, J. Karmouch, H.A. Katbi, X.J. Liu, Antiapoptotic role for ornithine decarboxylase during oocyte maturation. *Mol Cell Biol* 29, 1786-1795 (2009).

The wavelet-based denoising of images in Fiji/ImageJ, with example applications in structured illumination microscopy

Martin Čapek, Michaela Efenberková, Ivan Novotný, Ondrej Horváth

Introduction

Filtering super-resolved microscopic images is difficult. If we try to remove undesired image parts, e.g., noise, inhomogenous background, reconstruction artifacts, by standard filtration techniques, we lose resulting resolution that was acquired by hi-tech and expensive microscopy systems. Standard filtration methods include convolution-based techniques, like Gaussian smoothing, or Fourier-based techniques. These techniques suppose that noise and artifacts are small image parts that can be safely removed by some kind of convolution filtration, e.g., replacing a pixel intensity by a median intensity of this neighborhood, or by lowering the range of image frequencies in case of Fourier filtering. These techniques work nicely, e.g., for photographic images. However, these kinds of filtration do blur and increase the size of structures, which is not welcome in super-resolved microscopic images. Thus, another technique of image filtration that is able to preserve the size of structures and original resolution of microscopic images as much as possible would be desired.

One of promising and relatively modern techniques applied in digital image processing is a discrete wavelet transform (DWT). Discrete Fourier transform captures image frequencies. On the contrary, DWT captures both frequency and location information. In other words, DWT is able to distinguish, e.g., that one object in the picture is large and relatively intensity homogenous and other objects in the same picture are subtle with sudden intensity changes. Due to these properties, DWT is known to be interesting for the filtration of images.

There have been developed several tools for wavelet transformation of images till now. For example, interesting web-based demos were published (e.g., 1-3). First two links (1-2) demonstrate applying *Daubechies* and *Spline* based DWT to images, while the next one (3) does picture denoising by soft-thresholding in the wavelet domain.

Probably, the most efficient support for wavelet-based processing of signals and images has been implemented in *Matlab* (4) in its *Wavelet Toolbox*. Especially, *Wavelet Analyzer* tool is worth noting here. Other interesting tools aimed directly at denoising single images by orthonormal wavelet thresholding were presented in *Matlab* code (5, 6). *Matlab-based* libraries of third parties (*WavBox Software Library, WaveLab*) for wavelet analysis can be found here (7-8).

A standalone application for the study of the wavelet transform (*Visual Wavelet-Lab*) has been described (9), as well as simple applications for DWT – 2D *Fast Wavelet Transform Library* in C++ (10), *Wavelets* demo in *Accord.NET* framework

(11). *Xlib* library with DWT of images (12), *Fractional Wavelet Module* (2D or 3D) plugin with filtering possibilities (13), denoising single images using *Haar* filters (14) are, for example, possible in *ImageJ* (15).

Mostly, the above described approaches are mentioned as demos or relatively simple applications for DWT of images. The exceptions are tools in *Matlab*, which is, however, not a free software package and filtering of 2D/3D multichannel microscopic images of various formats is not straightforward with its using. Other exceptions are *Xlib* library of ImageJ plugins (12) that offers a tool for doing forward and backward DWT of images with various wavelet families, but without inherent filtering wavelet coefficients, and comprehensive *Fractional Wavelet Module* (2D or 3D) plugin (13) with various filter coefficients processing possibilities prior image synthesis, however, which is an older one and not offering some of the most common wavelet families used nowadays.

Thus, in our opinion, there is still missing a practical, freely available tool that does interactively DWT based filtering of large 2D/3D microscopic images using modern wavelet families.

Fiji is an open-source, freely available, image processing package (16). It is mentioned that it is a distribution of *ImageJ* (15) bundling many plugins which facilitate scientific image analysis. *Fiji* is a very popular choice of a program for image processing and analysis in microscopic research community. Plugins for *Fiji* can be easily developed by using *Java* and open-source integrated development environments, like *Eclipse* (18).

Therefore, we implemented a *Fiji/ImageJ* plugin called *Wavelet_Denoise*. The plugin follows a project and corresponding software *WTUTOR2D* that provides an educational tool for wavelet transform and its application in the field of digital image processing (17).

A stand-alone program *WTUTOR2D* is suitable for processing single grayscale images like photographs. It nicely demonstrates main possibilities of applying DWT to images: (i) Decomposition of an input picture to DWT using various wavelet filters and levels of details with decomposed image visualization; (ii) Effects of back transformation of the picture with the removal of a sub-band in the decomposed image; Effects of back transformation of the picture with some level of suppression (iii) or denoising (iv) of wavelet coefficients of the decomposed image. *WTUTOR2D* can be downloaded from (17).

Since we wished to provide large and worldwide *Fiji* community with interesting possibilities of *WTUTOR2D* software, we ported it from C# to Java, adapted to Fiji and created a plugin called *Wavelet_Denoise*. Advantages of the approach are that *Fiji* is able to read images using a plethora of various microscopic formats; *Fiji* users can easily install the plugin through a menu command; the plugin supports processing 3D images in Z-stacks; decomposed images can be stored in 32-bit format for analysis in other software packages (e.g., *Matlab*); approximation and detailed coefficients of DWT can be suppressed individually; and also

One-Slice-Preview for processing large 3D images is offered.

In this work we also demonstrate the application of the plugin and wavelet filtering for removal of reconstruction artifacts and undesirable background in images acquired by super-resolved structured illumination microscopy.

Discrete wavelet transform

For simplicity, we describe principles of DWT using a 1D signal (19). DWT uses a pair of filters, a low-pass filter *L* and a high-pass filter *H*. Using them we decompose the signal f of the length *N* into approximation coefficients *D* and detailed coefficients *A*. Since this filtering produces redundant data, *A* and *D* can be downsampled at half length. Subsequently, we would like to sample both of these signals (*A, D*) and filter them again using the reconstruction filters *L'* and *H'* to obtain the original signal after their composition (20). This procedure is illustrated in Fig. 1, where we first analyze (decompose) and then synthesize (reconstruct) the signal.
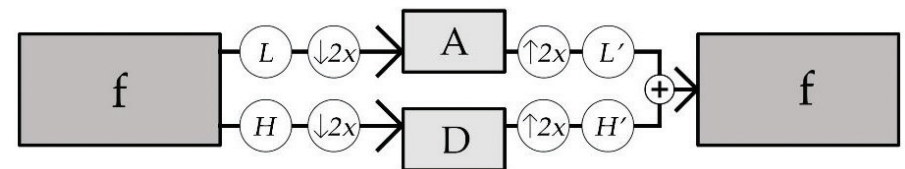

Figure 1. **Decomposition of the signal f into approximation and detailed coefficients A and D and subsequent synthesis of the original signal**
When analyzing the signal, we filter it using L and H and then subsample it. In the synthesis we upsample A and D and filter them using L' and H'. Finally, we add up both signals and get the original signal.

After the first analysis of signal f we can analyze the undersampled approximation coefficients *A* as well and divide them into the corresponding *A* and *D*. These can also be downsampled, as they contain redundant data, and we can iteratively repeat the analysis until the signal size permits. Then the original signal is reconstructed in a similar way (Fig. 2). This technique is called *subband* coding (20).
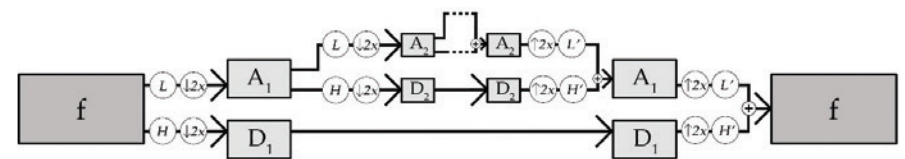

Figure 2. **Iterative analysis and subsequent signal synthesis** *A and D after the first iteration are A1 and D1, after the second iteration A2 and D2, etc.*

The filters *L* and *H* for analysis and *L'* and *H'* for signal synthesis must satisfy several conditions to ensure that the output signal matches the input. So-called orthogonal or biorthogonal filters meet the required conditions (20). There are many such filters in the literature, such as *Daubechies*, *Haar* or *Meyer* (20, 21, 22). In the way we have just described, i.e. by repeated filtration with suitable filters and resampling, we perform a wavelet transformation on a given signal in practice.

Example of DWT of a 2D signal is given in Fig. 3 which shows the original image as well as the transformed one. When transforming a 2D signal, we get approximation coefficients A (i.e., the downsampled image in the upper left corner of the transformed image) and series of detailed horizontal coefficients D^H (shown along the top horizontal edge of the image), detailed vertical coefficients D^V (along the left vertical edge) and detailed diagonal coefficients D^D (along the diagonal of the image).
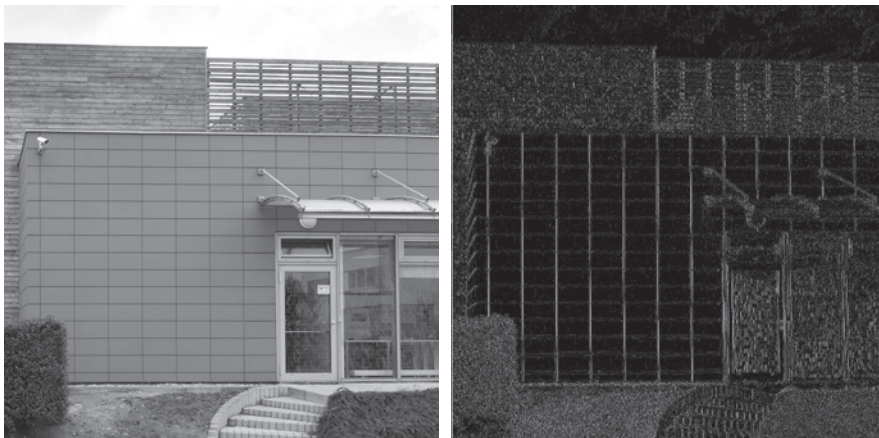

Figure 3. **Original 2D image (left) and its wavelet transformation using Daubechies 4 filters after three iterations (right)**
For better visualization, the transformed image values are linearly expanded and lines separating each frequency band are added.

When viewing the transformed image, it may be noted that the horizontal detail coefficients capture the intensity changes within the columns of the image, the vertical ones within the rows, and the diagonal within the diagonals. Moreover, with greater immersion we observe larger structures and coarser features of the image.

Structured illumination microscopy (SIM)

SIM is a super-resolution fluorescence light microscopy technique that breaks Abbé diffraction limit (23) and doubles resolution of standard fluorescence microscopes to about 100 nm (24). SIM uses sinusoidal illumination grid pattern to create moiré that carries information about details in specimens. For getting the image it is necessary to acquire usually fifteen pictures per one optical layer using three rotations and five shifts of the grid. The super-resolved image is reconstructed with the help of Fourier spectra analyses from the acquired pictures (25).

SIM is burdened by possible artifacts (26). Haloing is doubling structures in the reconstructed image. This is caused either by refractive index mismatch in the system of specimen, immersion oil and objective, or by photobleaching. It can be avoided by careful preparation of specimens, optimizing the refractive index of the immersion oil and avoiding bleaching across the specimen.

Another artifact observed in SIM is a regular, hexagonal pattern referred to as "honeycomb". It is common in pictures of specimens with low signal to noise ratio (SNR). This artifact is pronounced especially by masking the SIM pattern by high level of background and/or by using samples with diffuse labeling. This can be cured by visualizing samples that have discrete structures, i.e. that do not show diffuse labeling, by increasing SNR without photobleaching and by using appropriate parameters for SIM reconstruction, especially the Wiener filter constant.

However, although one is careful with sample preparation and acquisition, it may still happen that artifacts appear in the SIM data. Here comes the use of filtration.

Fiji/ImageJ plugin Wavelet_Denoise

When one runs the plugin in ImageJ, the following dialogs and pictures appear (Fig. 4).

The plugin works both with 2D images and with stacks (the first picture from the left in Fig. 4) and does processing in the wavelet domain – suppressing or denoising. It requires that 2D image dimensions are powers of two, otherwise, the plugin announces a warning message and stops.

It runs in three steps. Firstly, it computes the forward DWT (analysis, decomposition; the second picture from the left in Fig. 4). Secondly, it does an operation in the wavelet domain using a chosen wavelet filter and the level of details (Two *Levels of Detail, Haar, Soft Thresholding* applied in the main dialog in Fig. 4). Thirdly, it computes the inverse DWT from processed wavelet coefficients (synthesis, reconstruction; the third picture from the left in Fig. 4).

The dialog is modeless and accepts adjustments of the original image prior processing. Together with the plugin dialog and the pictures a *Synchronize Win-*
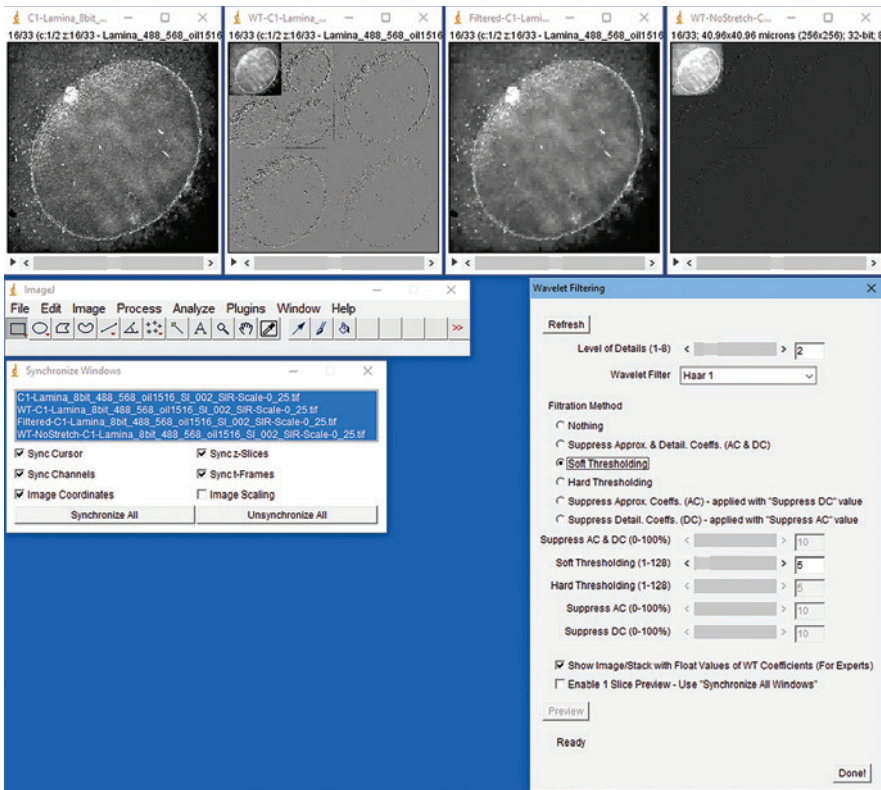
*Figure 4. **Screenshot of the Wavelet_Denoise plugin and images***

dows dialog appears that gives possibility to change image zoom easily, slice position etc. in all three pictures at once.

Level of Details can be chosen in the first slider. This means that we influence the depth of analysis and the following synthesis, as shown in Fig. 2. A relatively large set of wavelet filters has been implemented (*Haar, Daubechies* 1-20, *Symlets* 2-20, *Coiflets* 1-5, *Biorthogonal* 1.1-6.8, *Reverse Biorthogonal* 1.1-6.8, *Discrete Meyer*) and can be selected in the corresponding pop-up menu.

Processing (filtration) methods in the wavelet domain are offered in the group of radio buttons. *Nothing* means no processing is applied. Selecting *Suppress Approx. & Detail. Coeffs.* activates the corresponding slider (*Suppress AC & DC (0-100%)*) and removes chosen amount of ordered smallest coefficients. User sets the level of suppression that equals the percentage of the coefficients to be removed (i.e. 0% means no values are suppressed, 100% means all values are suppressed).

Denoise tools demonstrate the use of wavelet transform for image denoising. It is accomplished using thresholding (more specifically *VisuShrink* thresholding method) and the user defines the threshold by selecting the level of denoising (that equals Sigma value of the *Universal threshold*) in the dialog. It can also be selected to do either *Soft Thresholding* or *Hard Thresholding* (27).

Next two choices (*Suppress Approx. Coeffs. (AC), Suppress Detail. Coeffs. (DC)*) work together. Functionality is similar like in the option *Suppress Approx. & Detail. Coeffs.,* but both AC and DC are suppressed separately. Working together means that a user can, e.g., choose suppressing 10% of AC and 50% of DC and both suppressions are applied to the original picture.

When any parameter in the dialog is changed, both wavelet coefficients (the second picture in Fig. 4) and the reconstructed picture (the third one) are recomputed instantly. For standard images or stacks this can be acceptable, however, for large 3D stacks it may become time-consuming. For this purpose, we implemented *Enable 1 Slice Preview* option that gives possibility to set any parameter in the dialog without instant recomputation and after everything is set pressing the button *Preview* does the forward DWT, filtration and backward DWT for the actual slice only. Here it is recommended to use *Synchronize All Windows* to have simultaneous views to the same slice positions. When Enable 1 *Slice Preview* option is unchecked, the whole input image/stack is recomputed using the last parameters set.

The second picture in Fig. 4 represents a wavelet domain of the input picture. The image of the domain does not contain true values, but it is stretched to intensity range between 0 and 255 and optimized for visualization to easily see effects of suppressing or denoising. If a user wishes to get a picture of true coefficients, e.g., for next processing in *Matlab*, it is possible to check *Show Image/Stack with Float Values of WT Coefficients (For Experts)*. Then another picture with true real values of DWT will be open (the fourth one in Fig. 4).

By pressing the button *Refresh* is possible to return back to all default values of the main dialog together with corresponding recomputation of images. The dialog also shows an actual status or progress of computation in percent.

SIM data filtering examples

SIM works best with samples having discrete structures, like tubulin or actin networks in cells or pores in nuclei. When imaging samples with diffuse labeling and/or high background, the above mentioned "honeycomb" artefact, which is a regular, hexagonal pattern, often appears after reconstruction. This pattern negatively influences subsequent image analysis and processing.

We aimed to remove the reconstruction artefacts by using simple wavelet filtering. In the case of heavily artefacted SIM data it turned out that it is sufficient to decompose images using *Daubechies 4* wavelet and one level only. Afterwards, most noise and artefacts can be removed by restricting both approximation and detail coefficients to low values (Fig. 5-6).
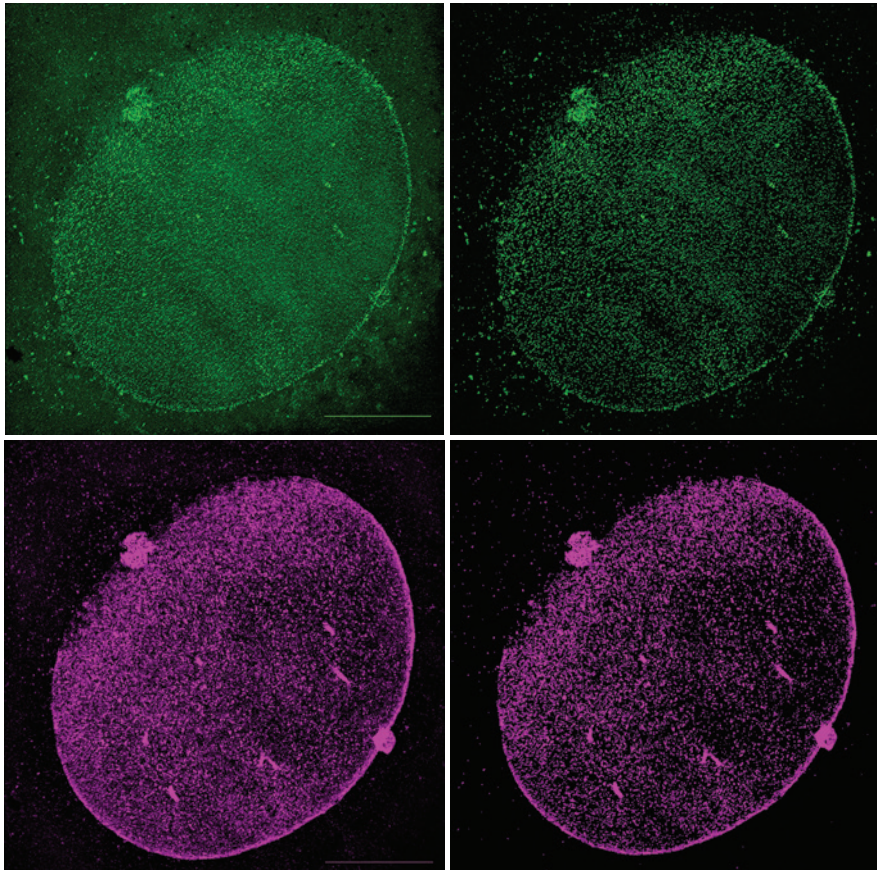
Figure 5. **Nuclear lamina, two fluorescence dyes, acquired by Nikon N-SIM:** *Green - exc/em 488/510 nm; Magenta - 568/590 nm. Left – original images, right – filtered images. Scale bars - 10 μm.*

Conclusions

Careful microscopic data acquisition is the best way to get high-quality images. However, it is not always possible. Then the filtration comes into play. Especially for images from super-resolved microscopes, we propose to apply *Wavelet_Denoise plugin* for *Fiji/ImageJ* that does filtration in the wavelet domain, with the advantage of preserving original resolution of the images. Since the content of images differs, image filtration is done interactively. After removing the honeycomb artifact, image analysis, e.g., colocalization, becomes more credible.
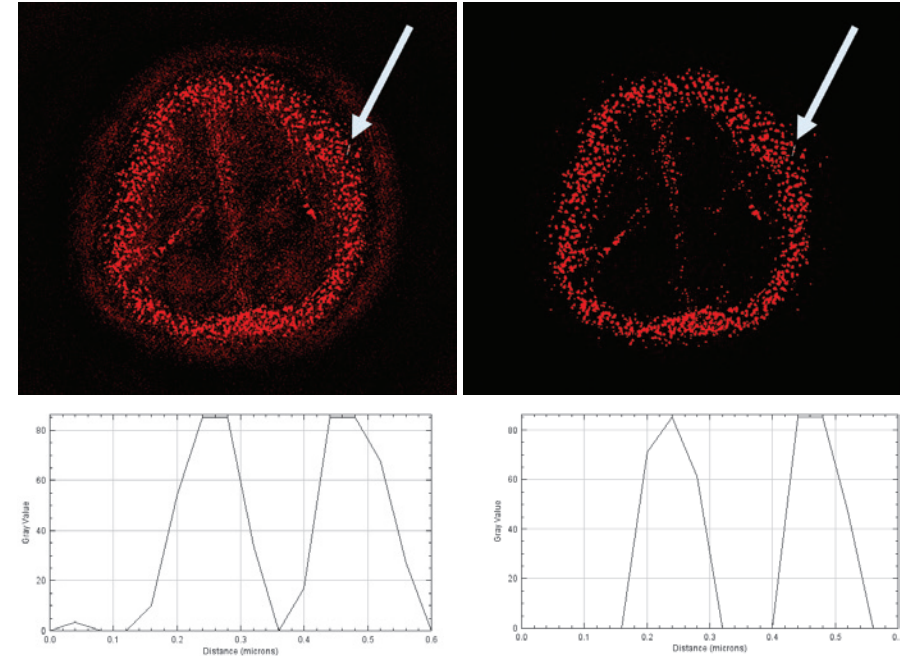

Figure 6. **Nuclear pores stained with AlexaFluor 555, acquired by Deltavision OMX 3D SIM: exc/em 555/590 nm** *Left – an original image, right – filtered image. Scale bar - 5 μm. Line profiles of two pores, see the arrows, demonstrate preserving resolution of the pores after filtration in the wavelet domain.*

References

1. http://bigwww.epfl.ch/demo/ip/demos/wavelets/
2. http://bigwww.epfl.ch/demo/ip/demos/wavelets-splines/
3. http://bigwww.epfl.ch/demo/ip/demos/wavelets-denoising/
4. https://www.mathworks.com/products/matlab.html
5. LUISIER, F., BLU, T., UNSER, M. A New SURE Approach to Image Denoising: Interscale Orthonormal Wavelet Thresholding. IEEE Transactions on Image Processing, vol. 16, no. 3, pp. 593-606, March 2007.

6. LUISIER, F., BLU, T. SURE-LET Multichannel Image Denoising: Interscale Orthonormal Wavelet Thresholding. IEEE Transactions on Image Processing, vol. 17, no. 4, pp. 482-492, April 2008.

7. https://www.toolsmiths.com/

8. http://statweb.stanford.edu/~wavelab/Wavelab_850/index_wavelab850.html

9. ROSELLÓ, E.G., DACOSTA, J.G., LADO, M.J., MÉNDEZ, A.J., SAMPEDRO J. and COTA, M.P. Visual Wavelet-Lab: An object-oriented library and a GUI application for the study of the wavelet transform. Computer Applications in Engineering Education. 2014, 22(1): 23-32.

10. https://www.codeproject.com/Articles/20869/D-Fast-Wavelet-Transform-Library-for-Image-Pro-ces

11. http://accord-framework.net/samples.html#

12. https://imagej.net/Xlib#Wavelets_2D

13. http://bigwww.epfl.ch/demo/fractsplines/java.html#module

14. https://imagej.nih.gov/ij/plugins/haar-wavelet-filter.html

15. https://imagej.nih.gov/

16. http://fiji.sc/

17. https://cbia.fi.muni.cz/software/wtutor2d.html

18. https://www.eclipse.org/

19. SEČKÁŘ, P. Educational tool for wavelet transform and its effective implementation using GPU (in Czech). Diploma work, 2015, FI MUNI Brno, 60 p.

20. STRANG, G. and T. NGUYEN. Wavelets and filter banks. Wellesley: Wellesley--Cambridge Press, c1997, xxi, 520 p. ISBN 09-614-0887-1.

21. GONZALEZ, R.C. and WOODS, R.E. Digital image processing. 3rd ed. Upper Saddle River, N.J.: Pearson Prentice Hall, c2008, xxii, 954 p. ISBN 978-013-5052-679.

22. CHUI, C. An introduction to wavelets. 1st ed. Boston: Academic Press, c1992, x, 264 p. ISBN 01-217-4584-8.

23. BORN, M. and WOLF, E. Principles of Optics. Cambridge University Press, 1997, ISBN 0-521-63921-2.

24. GUSTAFSSON, M.G.L. Surpassing the lateral resolution limit by a factor of two using structured illumination microscopy. Journal of microscopy, vol. 198 (nr. 2) p. 82-87, 2000. doi: 10.1046/j.1365-2818.2000.00710.x.

25. GUSTAFSSON, M.G.L, SHAO, L., CARLTON, P.M., WANG, C.J.R., GOLU-BOVSKAYA, I.N., CANDE, W.Z., AGARD, D.A. and SEDAT, J.W. Three-dimensional resolution doubling in wide-field fluorescence microscopy by structured illumination. Biophysical journal, vol. 94 (nr. 12) p. 4957-4970, 2008. doi: 10.1529/biophysj.107.120345

26. PELLET, P. Super-Resolution Imaging: SIM Capabilities, Sample Prep. & Analysis. GE Healthcare, Cell Analysis Workshop, May 6, 2015, PPT presentation.

27. RANGARAJAN, R., VENKATARAMANAN, R., SHAN, S. Image Denoising Using Wavelets: Wavelets & Time Frequency. University of Michigan, 2002.

Conditional gene deletion in the mouse lens by Cre/loxP system

Zbyněk Kozmik

Introduction

Vision is a crucial sense for vertebrates including humans. Vertebrate eye development is driven by a complex gene regulatory network which depends on the precise dosage and spatio-temporal expression of a suite of key transcription factors and signaling pathways (1). Perturbation of eye organogenesis, due to genetic factors, results in the lack of eye formation or various types of ocular diseases (2-5). Genetic manipulation in mice provides perhaps the best system to address the role that individual genes play during mammalian eye development. In such a way numerous genes that are involved in early steps of mouse eye development have been identified. Due to high evolutionary conservation these studies provided valuable mechanistic insight into the development of the human eye. Remarkably, parallel genetic studies in patient's cohorts identified mutations in corresponding human orthologues (2-5).

Morphogenesis of the vertebrate lens (Fig.1) is initiated when the evaginating optic vesicle outgrowing from the neuroepithelium of the developing brain induces overlying surface ectoderm consisting of columnar cells to form the lens placode. As development progresses, lens placode thickens and invaginates to form a hollow ball of epithelial cells, the lens vesicle. Invagination of the lens placode is highly coordinated with the invagination of optic vesicle to form optic cup. Cells located in the posterior lens vesicle elongate and differentiate into primary lens fiber cells, whereas anterior vesicle cells adopt a cuboid epithelial morphology (6). Lens grows rapidly during the late embryonic and neonatal stages by epithelial cell division and differentiation. In postnatal lenses, the cell division is restricted to the germinative zone of the epithelium at the equator and as these cells divide, they elongate and differentiate into the secondary fibers. Finally, in order to achieve lens transparency secondary fiber cells lose all the cellular organelles (6).

Genes that were shown to be required in early steps of eye development and lens organogenesis often encode transcription factors or components of the major signaling pathways. Most notably, paired and homeobox gene *Pax6* has been identified as a key ("master") regulator of eye development in both vertebrates and flies (7, 8). Human patients carrying a heterozygote mutation in *PAX6* gene suffer from various ocular anomalies, most notably aniridia (9). *Sey/Sey* mutant mice that are deficient in *Pax6* (10), completely lack eyes. Removal of *Pax6* gene function in the lens tissue leads to the arrest of lens induction (11), whereas retina-specific inactivation leads to a loss of multipotent character of retinal progenitor cells (12, 13). Overexpression of *Pax6* in *Xenopus* induces formation of